

Microscopic theory of antiferromagnetic and double superconducting transitions in UPt_3

This article has been downloaded from IOPscience. Please scroll down to see the full text article.

1994 J. Phys.: Condens. Matter 6 1749

(<http://iopscience.iop.org/0953-8984/6/9/016>)

View [the table of contents for this issue](#), or go to the [journal homepage](#) for more

Download details:

IP Address: 171.66.16.147

The article was downloaded on 12/05/2010 at 17:47

Please note that [terms and conditions apply](#).

Microscopic theory of antiferromagnetic and double superconducting transitions in UPt_3

A V Goltsev

Ioffe Physico-Technical Institute, Politechnicheskaya 26, St Petersburg 194021, Russia

Received 26 January 1993, in final form 30 April 1993

Abstract. The antiferromagnetic and double superconducting transitions in UPt_3 are studied by using a high-degeneracy model. Within the model, superconductivity is stimulated by long-range antiferromagnetic order. Two scenarios of the temperature behaviour are possible for the close-packed hexagonal structure. In the first scenario the double superconducting transition follows an antiferromagnetic transition ($T_{N1} > T_{c1} > T_{c2}$). In the second scenario the superconducting transition follows two consecutive antiferromagnetic transitions ($T_{N1} > T_{N2} > T_c$). For both scenarios the superconducting gap is anisotropic and vanishes along lines on the Fermi surface. The specific heat has the T^2 behaviour in the superconducting state.

1. Introduction

During the last few years much attention has been devoted to studying the properties of the heavy-fermion superconductor UPt_3 (see, for example, recent review papers [1, 2]). With decreasing temperature, the heavy-fermion, antiferromagnetic and superconducting states appear successively and coexist. The heavy-fermion state is formed by the coherent Kondo effect at temperatures below the Kondo temperature T_K . In this state electrons have enhanced mass $m^* \approx 200m_0$ near the Fermi surface [3]. Neutron-scattering experiments have revealed that an antiferromagnetic order arises at the Néel temperature $T_N = 5.5$ K [4, 5]. The corresponding antiferromagnetic structure is represented in figure 1. The moments of the U atoms in the state are anomalously small ($0.02 \mu_B$) [4, 5]. Then, at temperature $T_c \sim 0.5$ K the compound undergoes a superconducting transition [6]. Below T_c the antiferromagnetic order and superconductivity coexist. More detailed investigations have shown that there are two consecutive superconducting transitions [7]. Moreover, UPt_3 has a complete H - T phase diagram [7–10]. For the purpose of explaining the splitting of the superconducting transition, a phenomenological model based on the mutual influence of multicomponent d-type superconductivity and antiferromagnetism has been proposed and studied in detail [10–14].

The superconducting state of UPt_3 has unusual properties. In that state some physical parameters demonstrate a power-law temperature dependence, while the Bardeen–Cooper–Schrieffer (BCS) theory predicts a simple exponential law. For example, the observation of the T^2 dependence in the specific heat has been reported in [7, 15, 16]. Such a temperature behaviour of the specific heat can be related to an anisotropic superconducting gap, which vanishes along lines on the Fermi surface [17].

Unusual superconducting properties of UPt_3 and other heavy-fermion superconductors such as URu_2Si_2 , UBe_{13} and CeCu_2Si_2 have stimulated an active search for an unconventional mechanism of superconducting coupling. A detailed list of references on the problem may be found in [2].

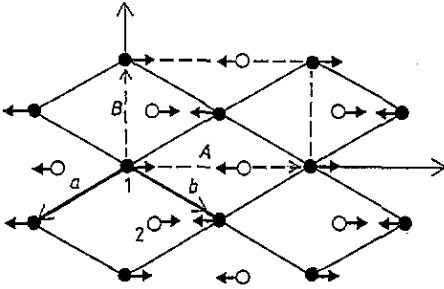


Figure 1. Positions of the U atoms in UPt_3 are represented by open and full circles in two adjacent planes, respectively. Arrows represent the moments of the U atoms. a and b are the translation vectors of the close-packed hexagonal structure. A and B are the translation vectors of the antiferromagnetic structure that arises at $T_N = 5.5$ K in UPt_3 [4, 5].

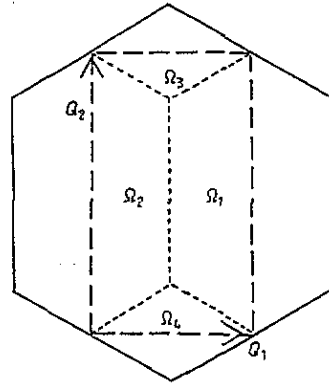


Figure 2. XY plane of the first Brillouin zone for the close-packed hexagonal structure. Dashed lines represent the reduced Brillouin zone corresponding to the antiferromagnetic structure of UPt_3 shown in figure 1. Q_1 and Q_2 are the reciprocal vectors of the antiferromagnetic structure. Dotted lines divide the reduced Brillouin zone into four regions Ω_1 , Ω_2 , Ω_3 and Ω_4 .

Recently I have proposed a new non-phonon mechanism of superconductivity for heavy-fermion superconductors [18]. I have found that long-range antiferromagnetic order appearing at $T_N < T_K$ can change the character of the local exchange interaction between conduction electrons and localized f electrons in such a way that at $T < T_N$ this interaction generates the superconducting coupling between heavy electrons near the Fermi surface. This mechanism of superconductivity leads to the anisotropic superconducting gap, which vanishes along lines on the Fermi surface [19]. Within the model I have also studied the properties of the antiferromagnetic state that precedes the superconducting transition. It has been found that the moments of rare-earth ions in the state are of the order $10^{-2} \mu_B$ in agreement with the experimental data.

In the present paper I apply the model to describe antiferromagnetic and superconducting transitions in heavy-fermion superconductors with the close-packed hexagonal structure. UPt_3 has such a structure, for example. For the structure the model predicts two possible scenarios of the temperature behaviour. In the first scenario an antiferromagnetic transition occurs first with decreasing temperature below the Kondo temperature T_K . Then, a double superconducting transition takes place, that is $T_{N1} > T_{c1} > T_{c2}$. In the second scenario two consecutive antiferromagnetic transitions occur first. Then, the system undergoes the superconducting transition ($T_{N1} > T_{N2} > T_c$). In both scenarios the superconducting state is characterized by an anisotropic gap, which is equal to zero on lines on the Fermi surface.

The paper is organized as follows. In section 2 the structure of the antiferromagnetic order in UPt_3 is analysed. In section 3, I study peculiarities of the antiferromagnetic state and the k dependence of the spin-density-wave (SDW) gap. I find that the system contains two antiferromagnetic instabilities. In section 4 it will be shown that these antiferromagnetic instabilities can stimulate two consecutive superconducting transitions. The particularities of the superconducting states and the k dependence of the superconducting gap are studied in section 4 also. Finally, section 5 contains some concluding remarks and a proposal for an experimental verification of the model under consideration.

2. Antiferromagnetic structure in UPt_3

UPt_3 has the close-packed hexagonal structure. Two adjacent planes of the structure are represented in figure 1. The corresponding translation vectors are

$$a = (-\frac{1}{2}\sqrt{3}a, -\frac{1}{2}a, 0) \quad b = (\frac{1}{2}\sqrt{3}a, -\frac{1}{2}a, 0) \quad c = (0, 0, c). \quad (2.1)$$

A unit cell of the structure contains two U atoms at positions

$$\rho_1 = (0, 0, 0) \quad \rho_2 = \frac{1}{3}a + \frac{2}{3}b + \frac{1}{2}c = (\frac{1}{6}\sqrt{3}a, -\frac{1}{2}a, \frac{1}{2}c). \quad (2.2)$$

In figure 1 the U atoms at these positions are denoted by numbers 1 and 2, correspondingly. The reciprocal vectors are

$$g_1 = 2\pi(-\sqrt{3}/3a, -1/a, 0) \quad g_2 = 2\pi(\sqrt{3}/3a, -1/a, 0) \quad g_3 = 2\pi(0, 0, 1/c). \quad (2.3)$$

Neutron-scattering measurements have revealed that a long-range antiferromagnetic order arising at $T_N = 5.5$ K has the structure represented in figure 1 [4]. The translation vectors of the antiferromagnetic structure are given by

$$A = b - a = (\sqrt{3}a, 0, 0) \quad B = -a - b = (0, a, 0) \quad C = c. \quad (2.4)$$

Consequently, the corresponding reciprocal vectors are

$$\begin{aligned} Q_1 &= \frac{1}{2}(g_2 - g_1) = 2\pi(\sqrt{3}/3a, 0, 0) \\ Q_2 &= -\frac{1}{2}(g_1 + g_2) = 2\pi(0, 1/a, 0) \\ Q_3 &= g_3. \end{aligned} \quad (2.5)$$

It may be easily shown that the unit-cell volume ($\Omega_a = |A \cdot B \times C|$) of the antiferromagnetic structure is twice as large as the unit-cell volume ($\Omega = |a \cdot b \times c| = \sqrt{3}a^2c/2$) of the initial lattice.

The first Brillouin zone of the close-packed hexagonal lattice looks like a prism with a regular hexagon as a basis (see figure 2). The antiferromagnetic order results in a reduction of the zone. The reduced Brillouin zone is a rectangular prism formed by reciprocal vectors (2.5). The volume of the reduced Brillouin zone is twice as small as the volume of the initial zone.

3. Antiferromagnetic ordering

I shall study antiferromagnetism and superconductivity of heavy-fermion compounds by using the Hamiltonian [18]

$$\begin{aligned} H_0 &= \sum_{\sigma k} \varepsilon_k c_{\sigma k}^+ c_{\sigma k} + \sum_{\sigma i} \varepsilon_i f_{\sigma i}^+ f_{\sigma i} - N^{-1/2} \sum_{\sigma i} V(b_i f_{\sigma i}^+ c_{\sigma i} + \text{HC}) + J_1 N^{-3} \sum_i S_{ci}^z S_{fi}^z \\ &\quad - J_2 N^{-1} \sum_{\sigma \eta i} f_{\sigma i}^+ c_{-\sigma i}^+ c_{-\eta i} f_{\eta i} \end{aligned} \quad (3.1)$$

where k is the wavenumber, the spin quantum numbers σ and η run from $-j$ to j , and $N = 2j + 1$ is the spin degeneracy. The sum over i is the sum over U atoms. The exchange constants J_1 and J_2 are supposed to be positive. The spin operators S_{fi}^z and S_{ci}^z are determined as

$$S_{fi}^z = \sum_{\sigma} \sigma f_{\sigma i}^{\dagger} f_{\sigma i} \quad S_{ci}^z = \sum_{\sigma} \sigma c_{\sigma i}^{\dagger} c_{\sigma i}. \quad (3.2)$$

Within the slave-boson method, the constraints

$$b_i^{\dagger} b_i + \sum_{\sigma} f_{\sigma i}^{\dagger} f_{\sigma i} = q_0 N \quad (3.3)$$

are imposed on each lattice site R_i .

In the framework of the mean-field approach, the effective Hamiltonian (H_{MF}) and mean-field free energy (F_{MF}) of the model under consideration are given by the following equations [18, 19]:

$$H_{MF} = \sum_{\sigma k} \varepsilon_k c_{\sigma k}^{\dagger} c_{\sigma k} + \sum_{\sigma i} [\varepsilon_{fi}^* f_{\sigma i}^{\dagger} f_{\sigma i} - V(r_{0i} f_{\sigma i}^{\dagger} c_{\sigma i} + \text{HC}) + J_1 N^{-1} (M_{ci} S_{fi}^z + M_{fi} S_{ci}^z) - (\Delta_i f_{\sigma i}^{\dagger} c_{-\sigma i}^{\dagger} + \text{HC})] \quad (3.4)$$

$$F_{MF} = -N \sum_i [J_1 M_{ci} M_{fi} - J_2^{-1} \Delta_i^* \Delta_i + (q_0 - r_{0i}^2) \lambda] - T \ln \text{Sp} \exp[-\beta (H_{MF} - \mu \hat{N}_t)] \quad (3.5)$$

where $\lambda \equiv \varepsilon_f^* - \varepsilon_f$, ε_f^* is the renormalized energy of the f level, μ is the chemical potential, and \hat{N}_t is the operator of the total number of electrons. The order parameters r_{0i} , M_{fi} , M_{ci} , Δ_i and the energy ε_f^* may be found by solving the equations

$$\begin{aligned} M_{fi} &= N^{-2} \langle S_{fi}^z \rangle & M_{ci} &= N^{-2} \langle S_{ci}^z \rangle \\ r_{0i} &= \frac{V}{N\lambda} \sum_{\sigma} \langle c_{\sigma i}^{\dagger} f_{\sigma i} \rangle & \Delta_i &= J_2 N^{-1} \sum_{\sigma} \langle c_{-\sigma i} f_{\sigma i} \rangle \\ \sum_{\sigma} \langle f_{\sigma i}^{\dagger} f_{\sigma i} \rangle &= N(q_0 - r_{0i}^2) \equiv N n_f \end{aligned} \quad (3.6)$$

where n_f is the occupancy of the f level per orbital. These equations result from the minimization of the free energy F_{MF} with respect to the order parameters.

I shall consider only the case when the Kondo temperature T_K is much larger than T_N and T_c . This enables us to neglect the effect of antiferromagnetic ordering and superconductivity on the parameters r_0 and ε_f^* that characterize the heavy-fermion state.

Let us study the properties of the antiferromagnetic state with the structure represented in figure 1. One can easily check that the antiferromagnetic order with wavevector Q_1 (2.5) corresponds to the antiferromagnetic structure. In the antiferromagnetic state we have

$$M_{f(c)i} = M_{f(c)} \cos(Q_1 R_i + \varphi_{f(c)}).$$

Therefore, the spin density wave is characterized by four parameters: two amplitudes M_f and M_c , and two phases φ_f and φ_c . However, it is more suitable to introduce four different parameters. One can write

$$M_{f(c)i} = M_{f(c)}(R_i) = M_{f(c)}(R_{nlm} + \rho_s) = M_{f(c)}^{(\sigma)} \cos Q_1 R_{nlm} \quad (3.7)$$

where $R_{nlm} = na + lb + mc$, and $R_i = R_{nlm} + \rho_s$ is the radius vector of the U atoms in the lattice. The vector ρ_s ($s = 1, 2$) is determined by equations (2.2). The quantities $M_f^{(1)}$ and $M_f^{(2)}$ are the moments of the U atoms at positions 1 and 2 within each unit cell (see figure 1). Since $\cos Q_l R_{nlm} = (-1)^{n+l}$, one can conclude that the antiferromagnetic structure (3.7) is equivalent to the structure represented in figure 1. $M_c^{(1)}$ and $M_c^{(2)}$ are the magnitudes of the spin density wave (SDW) formed by conduction electrons at the points ρ_1 and ρ_2 .

Substituting (3.7) into (3.4), one obtains the mean-field Hamiltonian describing the antiferromagnetic state:

$$H_{MF} = \sum_{l=1}^4 \sum_{\nu, \mu=1}^2 \sum_{\sigma} \sum_{k \in \Omega_l} [\delta_{\nu\mu} (E_{\nu k} b_{\nu\sigma k}^+ b_{\nu\sigma k} + E_{\nu p_l} b_{\nu\sigma p_l}^+ b_{\nu\sigma p_l}) + (A_{kp_l}^{\nu\mu} b_{\nu\sigma k}^+ b_{\mu\sigma p_l} + \text{HC})] \quad (3.8)$$

where k runs over regions Ω_l ($l = 1, \dots, 4$) of the reduced Brillouin zone (see figure 2). Moreover,

$$p_l \equiv k - q_l \quad q_1 \equiv Q_1 \quad q_2 \equiv -Q_1 \quad q_3 \equiv Q_2 \quad q_4 \equiv -Q_2 \quad (3.9)$$

$$A_{kp_l}^{\nu\mu} = \frac{\sigma}{N} J_1 \sum_{s=1,2} \exp(-iq_l \rho_s) (M_c^{(s)} v_{\nu k} v_{\mu p_l} + M_f^{(s)} u_{\nu k} u_{\mu p_l}). \quad (3.10)$$

The hybridized bands $E_{\nu k}$ ($\nu = 1, 2$) are determined by the equations

$$\begin{aligned} E_{1k} &= \frac{1}{2} \{ \varepsilon_k + \varepsilon_f^* - [(\varepsilon_k - \varepsilon_f^*)^2 + 4V^2 r_0^2]^{1/2} \} \\ E_{2k} &= \frac{1}{2} \{ \varepsilon_k + \varepsilon_f^* + [(\varepsilon_k - \varepsilon_f^*)^2 + 4V^2 r_0^2]^{1/2} \}. \end{aligned} \quad (3.11)$$

The annihilation operators $b_{\nu\sigma k}$ for quasiparticles in these bands are related to the operators $c_{\sigma k}$ and $f_{\sigma k}$ by the Bogoliubov transformation

$$\begin{aligned} c_{\sigma k} &= \sum_{\nu=1,2} u_{\nu k} b_{\nu\sigma k} & f_{\sigma k} &= \sum_{\nu=1,2} v_{\nu k} b_{\nu\sigma k} \\ u_{1k} &= v_{2k} = \cos \alpha_k & u_{2k} &= -v_{1k} = \sin \alpha_k \\ \cot \alpha_k &= (\varepsilon_f^* - E_{1k}) / V r_0. \end{aligned} \quad (3.12)$$

It is well known that the quasiparticles in the band E_{1k} near the Fermi surface have enhanced mass $m^*/m_0 = \cos^{-2} \alpha_F \sim 1/\rho_F T_k$, where ρ_F is the density of states on the Fermi surface.

In order to find the energy spectrum in the antiferromagnetic state, it is necessary to diagonalize the Hamiltonian (3.8). In accordance with [18] we have

$$\begin{aligned} \mathcal{E}_{1k\sigma} &= \frac{1}{2} \{ E_{1p} + E_{1k} - [(E_{1p} - E_{1k})^2 + 4|A_{kp}^{11}|^2]^{1/2} \} \\ \mathcal{E}_{2k\sigma} &= \frac{1}{2} \{ E_{1p} + E_{1k} + [(E_{1p} - E_{1k})^2 + 4|A_{kp}^{11}|^2]^{1/2} \} \\ \mathcal{E}_{3k\sigma} &= \frac{1}{2} \{ E_{2p} + E_{2k} - [(E_{2p} - E_{2k})^2 + 4|A_{kp}^{22}|^2]^{1/2} \} \\ \mathcal{E}_{4k\sigma} &= \frac{1}{2} \{ E_{2p} + E_{2k} + [(E_{2p} - E_{2k})^2 + 4|A_{kp}^{22}|^2]^{1/2} \} \end{aligned} \quad (3.13)$$

where $p = p_l$ if $k \in \Omega_l$.

I shall only consider the case when the total number of electrons ($n_t = n_c + n_f$) per orbital is smaller than $1/2$. It means that the lower antiferromagnetic band $\mathcal{E}_{1k\sigma}$ is partially full and the quasiparticles near the Fermi surface have enhanced mass. The antiferromagnetic transition opens a gap on those flat parts of the Fermi surface which are near the surface of the reduced Brillouin zone. Using (3.10) and (3.13), one obtains that the gap is

$$\Delta\mathcal{E}_1 = \Delta\mathcal{E}_2 = 2J_1 |(\sigma/N)| [(M_c^{(1)} + m_0 M_f^{(1)}/m^*)^2 + (M_c^{(2)} + m_0 M_f^{(2)}/m^*)^2 + (M_c^{(1)} + m_0 M_f^{(1)}/m^*)(M_c^{(2)} + m_0 M_f^{(2)}/m^*)]^{1/2} \quad (3.14)$$

in the regions Ω_1 and Ω_2 , and

$$\Delta\mathcal{E}_3 = \Delta\mathcal{E}_4 = 2J_1 |(\sigma/N)| [M_c^{(1)} - M_c^{(2)} + m_0 (M_f^{(1)} - M_f^{(2)})/m^*] \quad (3.15)$$

in the regions Ω_3 and Ω_4 . According to these equations, in the general case the SDW gap is anisotropic. A more detailed analysis of the anisotropy will be given below.

For the purpose of determining the Néel temperature and the structure of the antiferromagnetic state, let us consider an expansion of the free energy (3.5) in $M_{c(f)}^{(s)}$. The magnetic contribution of order $O(M^2)$ to the free energy per orbital and unit cell is

$$\mathcal{F}_m = -\frac{1}{2} J_1^2 \left\{ \frac{3}{4} \chi_f(Q_1) a_c^2 + \frac{3}{4} \chi_c(Q_1) a_f^2 + a_c a_f [F(Q_1) + J_1^{-1}] + \frac{1}{4} [\chi_f(Q_1) + 4\chi_f(Q_2)] b_c^2 + \frac{1}{4} [\chi_c(Q_1) + 4\chi_c(Q_2)] b_f^2 + b_c b_f [F(Q_2) + J_1^{-1}] \right\} \quad (3.16)$$

where

$$a_{c(f)} \equiv M_{c(f)}^{(1)} + M_{c(f)}^{(2)} \quad b_{c(f)} \equiv M_{c(f)}^{(1)} - M_{c(f)}^{(2)}. \quad (3.17)$$

The correlation functions $\chi_{c(f)}(Q)$ and $F(Q)$ are defined as

$$\begin{aligned} \chi_{c(f)}(Q) &\equiv T^{-1} N^{-3} \langle \langle S_{c(f)}^z(Q) S_{c(f)}^z(-Q) \rangle \rangle \\ F(Q) &\equiv T^{-1} N^{-3} \langle \langle S_c^z(Q) S_f^z(-Q) \rangle \rangle \end{aligned} \quad (3.18a)$$

where

$$S_c^z(Q_1) = \sum_{\sigma, k \in \Omega_1 + \Omega_2} \sigma c_{\sigma k}^+ c_{\sigma k - Q_1}, \quad S_c^z(Q_2) = \sum_{\sigma, k \in \Omega_3 + \Omega_4} \sigma c_{\sigma k}^+ c_{\sigma k - Q_2}. \quad (3.19)$$

In the temperature range $T_N < T < T_K$ the correlation functions (3.18a) may be written as

$$\begin{aligned} \chi_c(Q_l) &= \frac{j(j+1)}{6N^2} \sum_{\nu\mu} \sum_{k \in \tilde{\Omega}_l} u_{\nu k}^2 u_{\mu p}^2 \frac{\tanh(E_{\nu k}/2T) - \tanh(E_{\mu p}/2T)}{E_{\nu k} - E_{\mu p}} \\ \chi_f(Q_l) &= \frac{j(j+1)}{6N^2} \sum_{\nu\mu} \sum_{k \in \tilde{\Omega}_l} v_{\nu k}^2 v_{\mu p}^2 \frac{\tanh(E_{\nu k}/2T) - \tanh(E_{\mu p}/2T)}{E_{\nu k} - E_{\mu p}} \\ F(Q_l) &= \frac{j(j+1)}{6N^2} \sum_{\nu\mu} \sum_{k \in \tilde{\Omega}_l} v_{\nu k} v_{\nu p} u_{\mu k} u_{\mu p} \frac{\tanh(E_{\nu k}/2T) - \tanh(E_{\mu p}/2T)}{E_{\nu k} - E_{\mu p}} \end{aligned} \quad (3.18b)$$

where $\tilde{\Omega}_1 = \Omega_1 + \Omega_2$ and $p = k - Q_1$ for $l = 1$, and $\tilde{\Omega}_2 = \Omega_3 + \Omega_4$ and $p = k - Q_2$ for $l = 2$. It is important to note that the functions $\chi_{c(f)}(Q_1)$ and $F(Q_1)$ are determined only

by the energy spectrum in the regions Ω_1 and Ω_2 , whereas $\chi_{c(f)}(Q_2)$ and $F(Q_2)$ depend only on the energy spectrum in the regions Ω_3 and Ω_4 . In the limit $N \gg 1$ the functions $\chi(Q)$ and $F(Q)$ are of order $O(1)$. The character of the temperature behaviour of the functions (3.18b) may be easily found in the case when the Fermi surface contains flat parts that satisfy the nesting condition $E_{1k} - \mu = \mu - E_{1p}$ in the regions $\tilde{\Omega}_1$ and $\tilde{\Omega}_2$. One obtains that $\chi_{c(f)}(Q_1)$, $F(Q_1) \sim \ln(T_0/T)$ where T_0 is the low-temperature scale (for details see [18, 19]).

The Néel temperature may be found from the equation

$$\det|\partial^2 \mathcal{F}_m / \partial \lambda_i \partial \lambda_j| = 0 \quad (3.20)$$

where $\lambda_i = a_c, a_f, b_c, b_f$. Equation (3.20) has two solutions. The former corresponds to the formation of an antiferromagnetic state with $a_{c(f)} \neq 0$ and $b_{c(f)} = 0$, that is $M_{c(f)}^{(1)} = M_{c(f)}^{(2)}$ in accordance with (3.17). In other words, in this antiferromagnetic state the moments $M_f^{(1)}$ and $M_f^{(2)}$ of the U atoms at positions 1 and 2 within a unit cell (see figure 1) are the same. The corresponding Néel temperature T_{N1} is determined by the equation

$$4[1 + J_1 F(Q_1)]^2 = 9J_1^2 \chi_f(Q_1) \chi_c(Q_1). \quad (3.21)$$

The other solution corresponds to the formation of an antiferromagnetic state with $a_{c(f)} = 0$ and $b_{c(f)} \neq 0$, that is $M_{c(f)}^{(1)} = -M_{c(f)}^{(2)}$. The corresponding equation for the unrenormalized Néel temperature T_{N2} is

$$4[1 + J_1 F(Q_2)]^2 = J_1^2 [\chi_f(Q_1) + 4\chi_f(Q_2)][\chi_c(Q_1) + 4\chi_c(Q_2)]. \quad (3.22)$$

The antiferromagnetic structure observed in UPt_3 [4] and represented in figure 1 is the structure with $M_f^{(1)} = M_f^{(2)}$. That is why I shall only study the case $T_{N1} > T_{N2}$ that takes place if $\chi_{f(c)}(Q_1) > 2\chi_{f(c)}(Q_2)$. Using equations (3.14) and (3.15), one obtains that at T_{N1} the SDW gap is open only on those parts of the Fermi surface which lie in the regions Ω_1 and Ω_2 , i.e. $\Delta \mathcal{E}_{1,2} \neq 0$, $\Delta \mathcal{E}_{3,4} = 0$. In other words, in k -space the SDW gap does not open in directions normal to the wavevector Q_1 of the antiferromagnetic structure. Moreover, in the antiferromagnetic state the energy spectrum in the regions Ω_3 and Ω_4 is not renormalized, because at $M_{f(c)}^{(1)} = M_{f(c)}^{(2)}$ the parameter $A_{kp}^{v\mu}$ (3.10) at $p = k \pm Q_2$ is equal to zero and, consequently, $\mathcal{E}_{1k\sigma} = E_{1k}$ for $k \in \Omega_3, \Omega_4$.

In my previous papers [18, 19] it has been shown in the framework of model (2.1) that long-range antiferromagnetic order changes the character of the exchange interaction with the constant J_2 . This interaction brings about the superconducting coupling between heavy electrons near the Fermi surface. Therefore, with decreasing temperature there are two possible scenarios of the temperature behaviour. In the first scenario the superconducting transition occurs before the second antiferromagnetic transition, i.e. $T_{N1} > T_c > T_{N2}$. In the other scenario the second antiferromagnetic transition at T_{N2} follows the transition at T_{N1} . Then, the system undergoes at T_c the superconducting transition, i.e. $T_{N1} > T_{N2} > T_c$.

4. Double superconducting transition

First I shall consider the scenario $T_{N1} > T_c > T_{N2}$ and show that there are actually two consecutive superconducting transitions, $T_{N1} > T_{c1} > T_{c2}$.

In the superconducting state the local superconducting order parameter Δ_i (see equation (3.6)) becomes non-zero and has the following space dependence [18]

$$\Delta_i = \Delta(\mathbf{R}_i) = \Delta(\mathbf{R}_{nlm} + \rho_i) = \Delta^{(s)} \cos \mathbf{Q}_1 \mathbf{R}_{nlm}. \quad (4.1)$$

where $\Delta^{(1)}$ and $\Delta^{(2)}$ are the values of the local superconducting order parameter at positions 1 and 2 within each unit cell. After diagonalization of the Hamiltonian (3.8) described in [18], the mean-field Hamiltonian (3.4) is given by

$$\begin{aligned} H_{sc} = & \sum_{\sigma k} \mathcal{E}_{1\sigma k} a_{1\sigma k}^+ a_{1\sigma k} - \frac{1}{2} \sum_{\sigma} \sum_{k \in \Omega_1 + \Omega_2} [\Delta_{\sigma k}(\mathbf{Q}_1) a_{1\sigma k}^+ a_{1, -\sigma, -k}^+ + \text{HC}] \\ & - \frac{1}{2} \sum_{\sigma} \sum_{k \in \Omega_3 + \Omega_4} [\Delta_{\sigma k}(\mathbf{Q}_2) a_{1\sigma k}^+ a_{1, -\sigma, -k}^+ + \text{HC}] \end{aligned} \quad (4.2)$$

where

$$\begin{aligned} \Delta_{\sigma k}(\mathbf{Q}_1) = & -(\sigma/2N) J_1 (m_0/m^*)^{1/2} [3d(a_f - a_c) + g(b_f - b_c)] \\ & \times \cos[2\beta_k(\mathbf{Q}_1)] / (\mathcal{E}_{3k\sigma} - \mathcal{E}_{1k\sigma}) \end{aligned} \quad (4.3)$$

$$\Delta_{\sigma k}(\mathbf{Q}_2) = -(\sigma/2N) J_1 (m_0/m^*)^{1/2} g(b_f - b_c) \cos[2\beta_k(\mathbf{Q}_2)] / (\mathcal{E}_{3k\sigma} - \mathcal{E}_{1k\sigma}) \quad (4.4)$$

$$d \equiv \Delta^{(1)} + \Delta^{(2)} \quad g \equiv \Delta^{(1)} - \Delta^{(2)} \quad (4.5)$$

$$\cos[2\beta_k(\mathbf{Q})] = (E_{1p} - E_{1k}) / [(E_{1p} - E_{1k})^2 + 4|A_{kp}^{11}|^2]^{1/2}. \quad (4.6)$$

At T close to T_c the superconducting contribution $O(\Delta^2)$ to the free energy (3.5) per orbital and unit cell may be written as

$$\mathcal{F}_s = \frac{1}{2} J_2^{-1} (|d|^2 + |g|^2) - \frac{1}{16} [3d(a_f - a_c) + g(b_f - b_c)]^2 K(\mathbf{Q}_1) - |g|^2 (b_f - b_c)^2 K(\mathbf{Q}_2) \quad (4.7)$$

where

$$K(\mathbf{Q}_i) = \frac{J_1^2 m_0}{m^* N_u N^3} \sum_{\sigma} \sum_{k \in \Omega_i} \frac{\sigma^2 \cos^2[2\beta_k(\mathbf{Q}_i)] \tanh[\mathcal{E}_{1k\sigma} - \mu]/2T}{(\mathcal{E}_{3k\sigma} - \mathcal{E}_{1k\sigma})^2 (\mathcal{E}_{1k\sigma} - \mu)} \quad (4.8)$$

where N_u is the number of unit cells.

Let us determine the structure of the superconducting state and critical temperature T_c . The critical temperature T_{c1} of the first superconducting transition may be determined from the equation $\partial^2 \mathcal{F}_s / \partial d \partial d^* = 0$. Taking into account that, at $T < T_{N1}$, $a_{c(f)} \neq 0$ and $b_{c(f)} = 0$, this equation may be written as

$$\frac{9}{8} J_2 (a_f - a_c)^2 K(\mathbf{Q}_1) = 1. \quad (4.9)$$

In the general case the function $K(\mathbf{Q}_i)$ is proportional to $\ln(T_0/T)$ at low temperatures.

At $T < T_{c1}$ the superconducting state with $d \neq 0$ and $g = 0$ arises. It means, in accordance with (4.5), that $\Delta^{(1)} = \Delta^{(2)} \neq 0$. Below T_{c1} antiferromagnetism and superconductivity coexist. The superconducting transition opens the gap $|\Delta_{\sigma k}(\mathbf{Q}_i)|$ on the Fermi surface. Because at $T < T_{c1}$ the system is in the state with $M_{c(f)}^{(1)} = M_{c(f)}^{(2)}$ and $\Delta^{(1)} = \Delta^{(2)}$, equations (4.3) and (4.4) give $|\Delta_{\sigma k}(\mathbf{Q}_1)| \neq 0$ and $|\Delta_{\sigma k}(\mathbf{Q}_2)| = 0$. In

other words, the superconducting transition at T_{c1} opens the gap only on those parts of the Fermi surface which lie in the regions Ω_1 and Ω_2 of the reduced Brillouin zone. The rest of the Fermi surface remains ungapped. Because the superconducting state preserves the magnetic symmetry $M_{f(c)}^{(1)} = M_{f(c)}^{(2)}$, the energy spectrum in the regions Ω_3 and Ω_4 is still unrenormalized.

With decreasing temperature below T_{c1} the system under consideration can undergo another superconducting phase transition into a state with broken symmetry between the U atoms in the unit cell. To find the corresponding critical temperature T_{c2} , it is necessary to consider the quadratic expansion of the free energy (3.5) in parameters b and g . Using equations (3.16) and (4.7), one obtains

$$\mathcal{F}_{ms} = -\frac{1}{2}J_1^2\left\{\frac{1}{4}[\chi_f(Q_1) + 4\chi_f(Q_2)]b_c^2 + \frac{1}{4}[\chi_c(Q_1) + 4\chi_c(Q_2)]b_f^2 + b_c b_f [F(Q_2) + J_1^{-1}]\right\} \\ + \frac{1}{2}J_2^{-1}|g|^2 - \frac{3}{16}(a_f - a_c)(b_f - b_c)(d^*g + dg^*)K(Q_1). \quad (4.10)$$

Here the correlation functions $\chi_{c(f)}(Q_1)$ (3.18a) and $K(Q_1)$ must be calculated taking into account both antiferromagnetic order with $M_{f(c)}^{(1)} = M_{f(c)}^{(2)}$ and superconductivity with $\Delta_{\sigma k}(Q_1)$, because they are determined by integration over the regions Ω_1 and Ω_2 where the energy spectrum is strongly renormalized. In order to find $K(Q_1)$ it is necessary to replace in (4.8) the function $\mathcal{E}_{1k\sigma} - \mu$ by the function $[(\mathcal{E}_{1k\sigma} - \mu)^2 + |\Delta_{\sigma k}(Q_1)|^2]^{1/2}$. At $T < T_{c1}$ the functions are regular functions and decrease with decreasing temperature. However, the functions $\chi_{c(f)}(Q_2)$ and $F(Q_2)$ preserve the singular behaviour ($\sim \ln(T_0/T)$) determined by (3.18b), since the energy spectrum in the regions Ω_3 and Ω_4 is still unrenormalized.

It is interesting to note that the last term in equation (4.10) may be written as

$$-\frac{3}{8}[(M_f^{(1)} - M_c^{(1)})^2 - (M_f^{(2)} - M_c^{(2)})^2](|\Delta^{(1)}|^2 - |\Delta^{(2)}|^2)K(Q_1).$$

Thus, it looks like a contribution to the free energy arising due to coupling between antiferromagnetism and superconductivity in the phenomenological approach [10–14].

The critical temperature T_{c2} may be found from the equation $\det[\partial^2 \mathcal{F}_{ms} / \partial \lambda_i \partial \lambda_j] = 0$ where $\lambda_i = b_c, b_f, g, g^*$, which may be written in the form

$$4[1 + J_1 F(Q_2)]^2 = J_1^2[\chi_f(Q_1) + 4\chi_f(Q_2)][\chi_c(Q_1) + 4\chi_c(Q_2)] + \frac{9}{4}J_2(a_f - a_c)|d|^2 K^2 \\ \times (Q_1)\left\{\frac{1}{4}[\chi_f(Q_1) + \chi_c(Q_1)] + \chi_f(Q_2) + \chi_c(Q_2) + F(Q_2) + J_1^{-1}\right\}. \quad (4.11)$$

As discussed above, at $T < T_{c1} < T_{N1}$ the correlation functions $\chi_{c(f)}(Q_1)$ and $F(Q_1)$ are strongly renormalized, whereas the functions $\chi_{c(f)}(Q_2)$ and $F(Q_2)$ remain singular ($\sim \ln(T_0/T)$). This fact permits the existence of a solution of equation (4.11).

At $T < T_{c2}$ the magnetic order parameter $b_{f(c)} = M_{f(c)}^{(1)} + M_{f(c)}^{(2)}$ and superconducting order parameter $g = \Delta^{(1)} + \Delta^{(2)}$ simultaneously become non-zero. Therefore, in this state we have $M_f^{(1)} \neq M_f^{(2)}$ and $\Delta^{(1)} \neq \Delta^{(2)}$. It means that the second-order phase transition at T_{c2} disturbs both magnetic and superconducting symmetry between the U atoms within each unit cell.

It is interesting to note that equation (4.11) for T_{c2} differs from equation (3.22) for the unrenormalized critical temperature T_{N2} by the last term on the right-hand side. This term results from an interaction between magnetic and superconducting fluctuations. Moreover, since the term is positive, this interaction precipitates the transition at T_{N2} . One can classify the phase transition at T_{c2} as a mixed magnetic–superconducting transition. As I have shown above, the part of the Fermi surface lying in the regions Ω_1 and Ω_2 is gapped in the

temperature range $T_{N1} > T > T_{c2}$. The remaining part of the surface lying in the regions Ω_3 and Ω_4 is ungapped. The phase transition at T_{c2} opens both the SDW gap $\Delta\mathcal{E}_{3,4}$ and the superconducting gap $|\Delta_{\sigma k}(Q_2)|$ determined by equations (3.15) and (4.4), respectively, on the remaining part of the Fermi surface in the regions Ω_3 and Ω_4 of the reduced Brillouin zone.

Let us study the k dependence of the superconducting gap $|\Delta_{\sigma k}(Q)|$ at $T < T_{c2}$. The dependence is mainly determined by the function $\cos[2\beta_k(Q)]$ (see equations (4.3) and (4.4)). The function is equal to zero on the surface of the reduced Brillouin zone (the dashed lines on figure 2) where the following equalities hold: $E_{1k} = E_{1k-Q_1}$, $E_{1k} = E_{1k-Q_2}$. Let us consider an intersection between the Fermi surface ($\mathcal{E}_{1k\sigma} = \mu$) and the surface of the reduced Brillouin zone. In general, we obtain some lines along which we have $\cos(2\beta) = 0$. In accordance with (4.3) and (4.4) the superconducting gap $|\Delta_{\sigma k}(Q)|$ is also equal to zero along the lines. Such an anisotropy of the superconducting gap leads to the T^2 behaviour of the specific heat at $T < T_{c2}$ [17]. This theoretical result is in agreement with the specific-heat measurements for UPt_3 [7, 15, 16].

Now I briefly consider the other scenario ($T_{N1} > T_{N2} > T_c$) of the temperature behaviour of model (2.1). As discussed above in section 3, in the temperature range $T_{N1} > T > T_{N2}$ the system is in the antiferromagnetic state with $M_f^{(1)} = M_f^{(2)}$. This magnetic symmetry between the U atoms in positions 1 and 2 within each unit cell is broken at the critical temperature T_{N2} determined by equation (3.22) where $\chi_c(Q_1)$ and $\chi_f(Q_1)$ have to be calculated with account of non-zero $M_{c(f)}$, whereas the functions $\chi_{c(f)}(Q_2)$ and $F(Q_2)$ are still singular. An antiferromagnetic state with $M_f^{(1)} \neq M_f^{(2)}$ is formed below T_{N2} . The antiferromagnetic state stimulates a superconducting transition. The corresponding critical temperature T_c may be found by using the free energy (4.7) at $a_{c(f)} \neq 0$ and $b_{c(f)} \neq 0$:

$$\begin{aligned} [J_2^{-1} - \frac{9}{8}(a_f - a_c)^2 K(Q_1)] \{ J_2^{-1} - (b_f - b_c)^2 [2K(Q_2) + \frac{1}{8}K(Q_1)] \} \\ = \frac{9}{64}(a_f - a_c)^2 (b_f - b_c)^2 K^2(Q_1) \end{aligned} \quad (4.12)$$

where $K(Q)$ is determined by (4.8). At $T < T_c$ the superconducting state with superconducting order $\Delta^{(1)} \neq \Delta^{(2)}$ is formed and coexists with the antiferromagnetic state with $M_f^{(1)} \neq M_f^{(2)}$. The superconducting state has the same properties as the state at $T < T_{c2}$ in the first scenario discussed above.

5. Discussion and conclusion

In the present paper I have applied model (2.1) proposed in [18] for studying antiferromagnetic and superconducting states of a heavy-fermion compound with the close-packed hexagonal structure, such as UPt_3 . I have considered the antiferromagnetic and superconducting transitions that can occur at temperatures below the Kondo temperature T_K when the system is in the heavy-fermion state formed by the coherent Kondo effect. It has been shown that there are two possible scenarios of the temperature behaviour. In the first scenario there is one antiferromagnetic transition at T_{N1} and two consecutive superconducting transitions at T_{c1} and T_{c2} ($T_{N1} > T_{c1} > T_{c2}$). In the second scenario one superconducting transition follows two consecutive antiferromagnetic transitions ($T_{N1} > T_{N2} > T_c$). In order to understand the origin and structure of the antiferromagnetic and superconducting states, it is necessary to take into account that each unit cell of UPt_3 contains two U atoms at positions 1 and 2, which lie in two adjacent atomic planes (see figure 1

and equation (2.2)). The successive antiferromagnetic and superconducting transitions are related to two different groups of electrons. Only the electrons with wavenumber k lying in the regions Ω_1 and Ω_2 of the reduced Brillouin zone (see figure 2) participate in the antiferromagnetic and superconducting transitions occurring at T_{N1} and T_{c1} , respectively, and preserving the symmetry between the U atoms in each unit cell. The other group of electrons with k lying in the regions Ω_3 and Ω_4 takes part in the second superconducting or second antiferromagnetic transitions, which disturb the symmetry.

In the first scenario the antiferromagnetic structure represented in figure 1 appears at T_{N1} . In the antiferromagnetic state the magnetic moments of the U atoms at positions 1 and 2 within each unit cell are the same ($M_f^{(1)} = M_f^{(2)}$). The antiferromagnetic transition opens a gap on a portion of the Fermi surface. If the portion is sufficiently small, then the jump in the specific heat at T_{N1} may be too small to be observed in specific-heat measurements. In my previous papers [18, 19] it has been shown that the magnetic moments of rare-earth atoms in the antiferromagnetic state are of order $10^{-2} \mu_B$, in agreement with the experimental data [4, 5].

With decreasing temperature below T_{N1} long-range antiferromagnetic order stimulates at T_{c1} the superconducting transition due to the non-phonon mechanism proposed in [18]. Below T_{c1} the superconductivity manifests itself in non-zero local order parameter Δ_i (see equation (3.6)). Although the order parameter looks like superconducting coupling between the conduction electrons and f electrons, in reality the non-zero order parameter Δ_i results from the superconducting coupling between heavy quasiparticles in the lower antiferromagnetic band. These heavy quasiparticles are the hybridized particles formed by f electrons, giving the main contribution, and conduction electrons (see equation (3.12)). Below T_{c1} the anomalous correlation function $\langle a_{1\sigma k}(\tau) a_{1,-\sigma,-k}(\tau') \rangle$ becomes non-zero and looks like the conventional anomalous correlation function with k -dependent superconducting order parameter Δ_k . Relating the local order parameter Δ_i with the anomalous correlation function, one obtains the equation determining Δ_k [19].

In the superconducting state the local superconducting order parameter Δ_i is modulated by the antiferromagnetic wavevector Q_1 in such a way that the values of Δ_i at positions 1 and 2 within each unit cell are the same ($\Delta^{(1)} = \Delta^{(2)}$). The superconducting gap is open only on those parts of the Fermi surface which lie in the regions Ω_1 and Ω_2 of the reduced Brillouin zone shown in figure 2. The rest of the surface remains ungapped. Such an anisotropic character of the superconducting gap may be revealed by measuring, for example, the angular dependence of the ultrasonic attenuation in the temperature range $T_{c1} > T > T_{c2}$. However, for that purpose it is necessary to have a single-domain sample. The anisotropy may be smeared in polydomain samples.

The second order phase transition at T_{c2} breaks down the symmetry between the U atoms within each unit cell. Below T_{c2} the magnetic moments of these two U atoms and the values of the local superconducting order parameter at the atoms have different magnitudes ($M_f^{(1)} \neq M_f^{(2)}$, $\Delta^{(1)} \neq \Delta^{(2)}$). The breakdown of the symmetry leads to the appearance of both SDW and superconducting gaps on the remaining part of the Fermi surface lying in the regions Ω_3 and Ω_4 of the reduced Brillouin zone. The phase transition at T_{c2} may be classified as a mixed magnetic-superconducting transition. The formation of the state with $M_f^{(1)} \neq M_f^{(2)}$ at $T < T_{c2}$ may be revealed by using neutron-scattering measurements, for example. The coupling between antiferromagnetism and superconductivity has been observed in [20]. Is the effect equivalent to the breakdown of the magnetic symmetry between the U atoms within each unit cell predicted by the model (2.1)? Further experimental and theoretical studies are necessary to give an answer to the question.

I have found also that at $T < T_{c2}$ the superconducting gap is anisotropic and vanishes

along lines on the Fermi surface. Consequently, the specific heat has T^2 behaviour at T below T_{c2} .

The system under consideration can also demonstrate the other scenario of the temperature behaviour: $T_{N1} > T_{N2} > T_c$. In the temperature range $T_{N1} > T > T_{N2}$ the system is in the antiferromagnetic state with $M_f^{(1)} = M_f^{(2)}$. The magnetic symmetry is broken down by the phase transition at T_{N2} . Below T_{N2} the antiferromagnetic state with $M_f^{(1)} \neq M_f^{(2)}$ arises. Only one superconducting transition can occur in the antiferromagnetic state. The superconducting state at $T < T_c$ has the same properties as the state appearing below T_{c2} in the first scenario.

In the present paper I have not studied the magnetic field effect on the phase diagram of model (2.1). Thus, the question about the H - T phase diagram still remains open.

References

- [1] De Visser A, Menovsky A and Franse J J M 1987 *Physica B & C* **147** 81
- [2] Grewe N and Steglich F 1991 *Handbook on the Physics and Chemistry of Rare Earths* vol 14, ed K A Gschneider Jr and L Eyring (Amsterdam: North-Holland) p 343
- [3] Chen J W, Lambert S E, Maple M B, Fisk Z, Smith J L, Stewart G R and Willis J O 1984 *Phys. Rev. B* **30** 1583
- [4] Aeppli G, Bucher E, Goldman A I, Shirane G, Broholm C and Kjems J K 1988 *J. Magn. Magn. Mater.* **76 & 77** 385
- [5] Aeppli G, Bucher E, Broholm C, Kjems J K, Baumann J and Hufnagl J 1988 *Phys. Rev. Lett.* **60** 615
- [6] Steart G R, Fisk Z, Willis J O and Smith J L 1984 *Phys. Rev. Lett.* **52** 679
- [7] Fisher R, Kim S, Woodfield B, Phillips N, Taillefer L, Hasselbach K, Flouquet J, Giorgi A and Smith J 1989 *Phys. Rev. Lett.* **62** 1411
- [8] Müller V, Roth C, Maurer D, Scheidt E, Lüders K, Bucher E and Bömmel H 1987 *Phys. Rev. Lett.* **58** 1224
- [9] Schenstroem A *et al* 1989 *Phys. Rev. Lett.* **62** 332
- [10] Thalmeier P, Wolf B, Weber D, Bruls G, Lüthi B and Menovsky A A 1991 *Physica C* **175** 61
- [11] Joynt R 1988 *Supercond. Sci. Technol.* **1** 210
- [12] Hess D W, Tokuyasu T and Sauls J A 1989 *J. Phys.: Condens. Matter* **1** 8135
- [13] Machida K, Ozaki M and Ohmi T 1989 *J. Phys. Soc. Japan* **58** 4116
- [14] Mineev V P 1991 *Physica B* **171** 138
- [15] Franse J J M, Menovsky A, de Visser A, Bredl C D, Gottwick U, Lieke W, Mayer H M, Rauchschalbe U, Sporn G and Steglich F 1985 *Z. Phys. B* **59** 15
- [16] Sulpice A, Gandit P, Chaussy J, Flouquet J, Jaccard D, Lejay P and Tholence J L 1986 *J. Low Temp. Phys.* **62** 39
- [17] Volovik G E and Gorkov L P 1985 *Zh. Eksp. Teor. Fiz.* **88** 1412 (*Sov. Phys.-JETP* **61** 843)
- [18] Goltsev A V 1992 *J. Phys.: Condens. Matter* **4** L447
- [19] Goltsev A V *Physica B* submitted
- [20] Aeppli G, Bishop D, Broholm C, Bucher E, Siemensmeyer K, Steiner K and Stüsser N 1989 *Phys. Rev. Lett.* **63** 676